ACS Catalysis

Research Article

pubs.acs.org/acscatalysis

Selective Degenerative Benzyl Group Transfer in Olefin Polymerization

Silei Xiong,[†] D. Keith Steelman,[‡] Grigori A. Medvedev,[†] W. Nicholas Delgass,[†] Mahdi M. Abu-Omar,*[,†,‡] and James M. Caruthers*[,†]

[†]School of Chemical Engineering, Purdue University, Forney Hall of Chemical Engineering, 480 Stadium Mall Drive, West Lafayette, Indiana 47907, United States

[‡]Brown Laboratory and the Negishi Brown Institute, Department of Chemistry, Purdue University, 560 Oval Drive, West Lafayette, Indiana 47907, United States

Supporting Information

ABSTRACT: The kinetics of 1-hexene polymerization was investigated using a previously studied zirconium amine bis-phenolate catalyst, Zr[tBu-ON^{THF}O]Bn$_2$, where the effect of substoichiometric amounts of activator on the polymerization was studied to more clearly elucidate the mechanism of degenerative benzyl-group transfer. Comprehensive kinetic analysis was performed for a diverse set of data including monomer consumption, evolution of molecular weight, and end-group counts over a range of activator to precatalyst ratios, where the analysis determined the rates of association and dissociation of a binuclear complex (BNC) intermediate through which degenerative transfer proceeds. Kinetic modeling indicates that the benzyl-group transfer inside the BNC is rapid, as supported by ^{1}H NMR. Rapid association and dissociation of the BNC enable complete activation of all precatalysts even under the condition of substoichiometric amounts of activator through a degenerative benzyl-group transfer. Through the use of a novel experimental technique wherein a labeled catalyst is introduced during a normal polymerization reaction, this process has been observed to instantaneously activate all incoming precatalyst and effectively shut down the misinsertion pathway. The kinetic analysis shows that BNC has a faster initiation rate than a typical catalyst−ion pair, which may be due to the anion being previously displaced by the incoming unactivated precatalyst.

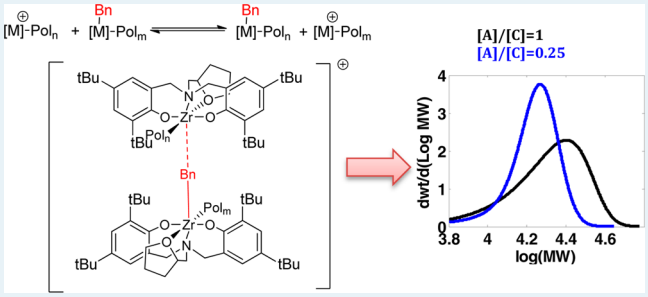

KEYWORDS: *degenerative transfer, 1-hexene, polymerization, kinetic modeling, catalysis*

INTRODUCTION

Because of the opportunity for more precise control of the polymer's molecular architecture, homogeneous single-site catalysts have attracted considerable attention.[1−3] The precatalysts can be activated by a number of activators to generate a coordinately unsaturated cation with an associated counteranion, a zwitterionic catalyst,[4] where the activators include methyl-aluminoxane (MAO), tris-(pentafluoro phenyl) borane ($B(C_6F_5)_3$, and perfluoroarylborate ($[BAr^F_4]^-$) and aluminate salts.[5] However, unlike MAO, which produces multiple and sometimes ambiguous catalytic species, $B(C_6F_5)_3$- and $[BAr^F_4]^-$-based activators activate these complexes in a stoichiometrically precise fashion,[6] enabling fundamental kinetic analysis.

The traditional mechanism for single-site polymerization involves activation, initiation, propagation, and finally chain transfer and/or termination.[7] However, the polymerization may also include degenerative transfer, where an actively polymerizing chain reacts with a dormant chain thereby reactivating the dormant chain for additional polymerization. The concept of degenerative transfer has been previously employed in the analysis of anionic, cationic, group transfer, and controlled/living free radical polymerizations.[8−11] For systems where the exchange between active and "dormant" groups is slow compared to propagation, the resulting molecular weight is broadened compared to analogous systems where degenerative transfer does not occur.[8,9] Conversely, when the rate constant for degenerative transfer is much greater than the rate constant for propagation (i.e., $k_{ex} \gg k_p$), the molecular weight distribution of the resulting polymer is narrow, and the undesired effects of bimolecular reactions are minimized or eliminated.[12]

It has been shown that under conditions where the activator is limiting, Group IV metallocene complexes have a tendency to form dimeric species due to competition between the $[BAr^F_4]^-$ counteranion and the neutral, unactivated metallocene complex for the highly electrophilic activated metallocene cation.[9,12−14] The mechanistic implication is that cooperativity can provide

Received: January 7, 2014
Revised: February 26, 2014
Published: February 28, 2014

   dx.doi.org/10.1021/cs500021g | ACS Catal. 2014, 4, 1162−1170

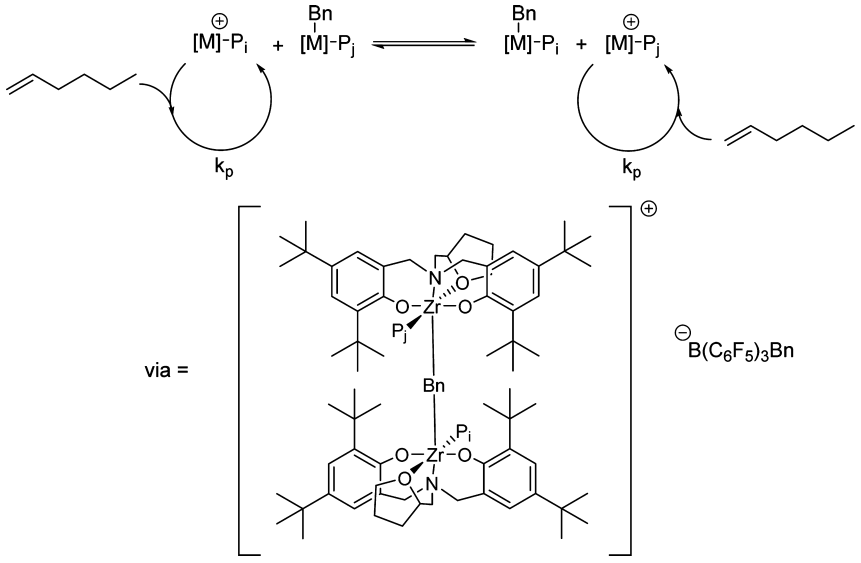

Figure 1. 1-Hexene polymerization catalyzed by zirconium salan-type catalyst Zr[tBu-ON(THF)OBn$_2$ using substoichiometric amounts of tris(pentafluorophenyl) borane. The structure of the precatalyst is published in previous work.[7b]

an additional variable for the control of important aspects of single-site polymerization catalysis, including stereocontrol.[13a] This cooperative effect has been exploited in the development of multinuclear single-site catalysts, which offer the possibility of creating novel polymeric architectures beyond the reach of conventional mononuclear catalytic systems, including ethylene−styrene copolymerization[13b] and enhanced methyl chain branching.[13c]

Much of the mechanistic work concerning binuclear interactions has focused on the systems containing two nontethered metal centers. Bochmann and Lancaster observed peak broadening of Zr-Me ^{1}H NMR signal in a series of $[Cp_2MR_2]$ (R = alkyl, M = Ti, Zr, or Hf)/ $[CPh_3][B(C_6F_5)_4]$ systems that they interpreted as a signature of the formation of a binuclear complex (BNC).[15] The BNC arises from the interaction of an actively polymerizing metal center with a neutral metal center from precatalyst, where the neutral metal center is, in essence, activated by the active metal−ligand complex, leaving the former in a neutral state with the general structure X−M−P (X = an abstractable group, M = metal, and P = polymer).[9,12] Marks and co-workers reported the formation of BNC by constrained geometry catalysts as indicated by NMR broadening.[14]

Sita and co-workers recently reported a detailed study of the degenerative ligand transfer in olefin polymerization using mixed metallocene acetamidinate catalysts with a substoichiometric amount of activator, where they employed the concept of a BNC.[12] In this study, a ^{13}C-enriched catalyst was used to observe the methyl exchange and metal-centered epimerization, which led to the postulate of the BNC. Studying activity and the MWD at the end of the reaction, Sita and co-workers observed that (1) the rate of consumption linearly decreased with increase in the amount of precatalyst while keeping the activator concentration constant, (2) the M_n was determined by only the monomer to precatalyst ratio and not the amount of the activator, and (3) the PDI was independent of the excess amount of precatalyst.[12a] Using the model proposed by Muller and co-workers,[9] Sita et al. argued that the mechanism consistent with these observations must include the rate of BNC formation that is much faster than k_p (propagation) and the equilibrium constant for BNC formation that is much larger than the observed consumption rate. It should be pointed out that the work of Sita et al., although containing the aforementioned qualitative conclusions about relative rates of the BNC-related reactions, did not produce the actual rate constants. The system studied by Sita and co-workers is essentially living, where the PDI value is less than 1.05. On the other hand, most of the group IV single-site catalysts are not living. For example, a significant amount of misinsertion occurs in the Salan catalyst systems.[7] It would be instructive from both a practical and fundamental standpoint to study if the BNC formation happens similarly if the polymeric species involved are normally inserted or misinserted. Furthermore, occurrence of the BNC discussed above has been limited until now to methyl or chloride abstractable groups. In fact, it has been stated specifically that the benzyl ligand could not form the BNC.[15]

We have previously studied the polymerization kinetics for a family of group IV amine bis-phenolate (salan)-ligated precatalysts, which is characterized by high activity and solubility in conventional organic solvents like toluene.[16,17] The complete kinetic analysis of this system under stoichiometric activator to precatalyst ratio has been carried out,[7b] where we have used our previously established techniques[7] to robustly determine the mechanism and rate constants for all of the elementary steps. In particular, we have found that the Zr[^{t}Bu-ON^{THF}O]Bn$_2$/B(C$_6$F$_5$)$_3$ catalyst system possesses a relatively large amount of misinsertion, where the concentration of the secondary (i.e., 2,1-misinserted) active sites under typical conditions equals the concentration of the primary (i.e., normally 1,2-inserted) active sites. As such, this system represents an attractive candidate for a study of BNC formation by different active sites, provided the BNC formation can be effected.

In this study, we report the polymerization kinetics of the Zr[^{t}Bu-ON^{THF}O]Bn$_2$/B(C$_6$F$_5$)$_3$ catalyst system under substoichiometric activator conditions in order to elucidate the degenerative transfer process. We will first demonstrate BNC formation for this system via peak broadening of the Zr-benzyl ^{1}H NMR signal. Next, we will show that the change in the

dx.doi.org/10.1021/cs500021g | ACS Catal. 2014, 4, 1162−1170

MWD with decreasing amounts of activator cannot be explained using the mechanism established under the condition of a stoichiometric amount of activator. In light of the aforementioned literature claim that the benzyl bridged BNC cannot form,[15] we undertook the task of elucidating the mechanism capable of describing the data. A sequence of increasingly complex kinetic mechanisms has been analyzed, where a minimal mechanism set capable of predicting the data in its entirety has emerged as the one that involves the formation of BNC (Figure 1). In addition to kinetic analysis, we will provide additional experimental evidence for the formation of the BNC via a novel experimental procedure where a labeled catalyst is introduced when the polymerization reaction is approximately 50% completed. Most importantly, the kinetic mechanism arrived upon in this study implies that the BNC formation is highly selective in that the BNC can only be formed by the coupling between the primary active sites and neutral precatalytic species and not by the secondary misinserted active sites. This selectivity has an additional benefit of producing polymer with narrow MWD.

The ability to quantitatively fit the multiresponse data provides confidence in that this minimal kinetic model is a robust description of the underlying polymerization process. The comprehensive kinetic modeling of Zr[^{t}Bu-ON^{THF}O]Bn_2/$B(C_6F_5)_3$ system also enables extraction of the rate constants of association and dissociation of the BNC, which clearly indicate that the actual benzyl-group transfer is rapid. Another interesting feature that results from the kinetic modeling of this system is that the BNC has a faster initiation rate than the zwitterion pair catalyst. This is likely due to the anion being previously displaced by the incoming unactivated precatalyst.

In recent years, considerable attention has been paid to the development of novel processes that reduce or eliminate the need for an activator.[12,13,18] As a result of decreasing the amount of activator present in the system, there is an increase in cooperativity between two distinct metal centers which gives rise to new mechanistic possibilities and increased polymerization control.[12,13] The BNC complex has the added benefit of simultaneously activating all neutral precatalyst molecules contained in the system using a minimal amount of activator.

EXPERIMENTAL PROCEDURE

General Procedure. All manipulations were performed under inert atmosphere in a glovebox or on a vacuum manifold. Toluene and pentane were purified over activated alumina and a copper catalyst using a solvent purification system (Anhydrous Technologies), degassed through freeze−pump−thaw cycles, and stored over activated molecular sieves. Tetrabenzylzirconium was purchased from STREM and used as received. 1-Hexene was purchased from Aldrich, purified by distillation over a small amount of $CpZrMe_2$, and stored over molecular sieves. $B(C_6F_5)_3$ was purchased from STREM and purified by sublimation. Diphenylmethane was purchased from Aldrich and stored over molecular sieves. CD_3OD was purchased from Cambridge Isotopes and used as received. d_8-Toluene was used as received and stored over molecular sieves. ^{1}H and ^{2}H NMR experiments were performed on a Varian INOVA600 MHz or Bruker DRX500 MHz spectrometer.

The ligand and unlabeled precatalyst were prepared following literature procedures.[7,16,17,19]

Quenched NMR Scale Polymerization of 1-Hexene. To a catalyst/activator solution in an NMR tube at 25 °C, 1-hexene was added. At the desired monomer conversion, this reaction was quenched with 0.75 mL of d_4-CD_3OD. These reactions were quenched at the desired conversion of monomer using 0.75 mL of d_4-methanol. The quench reaction was analyzed as previously described.[7]

Zr[tBu-ON^{THF}O]Cl_2 Synthesis. $ZrCl_4$ (3.6141 g, 15.5 mmol) and 25 mL of ether were added to a 100 mL flask. In a separate flask, 25 mL of ether and tBu-ON^{THF}O ligand (8.3408 g, 15.5 mmol) were added. Each flask was allowed to cool to −30 C. The ligand solution was then added to the $ZrCl_4$ slowly. The resulting colorless solution was filtered, and the white solid was discarded. The leftover solution was dried under vacuum to yield a colorless solid (93% yield). The solid is >95% pure, by ^{1}H NMR. No further purification was needed.

Zr[tBu-ON^{THF}O]d_7-Bn_2 Synthesis. Zr[tBu-ON^{THF}O]Cl_2 (2.10 g, 3.0 mmol) and 25 mL of d_8-toluene were added to a 100 mL flask. This flask was allowed to cool to −30 C. To this flask, solid d_7-benzylpotassium (1.65 g, 12.0 mmol) was added. The reaction mixture was allowed to warm up to 25 °C over 30 min. Then, the reaction mixture was heated to 60 °C for 2 h. The resulting slurry was treated with 30 mL of dichloromethane and filtered yielding a yellow solution. The solution was dried under vacuum to give a yellow solid (63% yield). The solid was found by ^{1}H NMR and ^{2}H NMR to be >95% pure product. The solid was recrystallized in d_8-toluene to yield an analytically pure complex.

Batch Polymerization of 1-Hexene Using Zr[tBu-ON^{THF}O]Bn_2 with an Additional Equivalent of Labeled Zr[tBu-ON^{THF}O]d_7-Bn_2. Zr[tBu-ON^{THF}O]Bn_2 (0.073 g, 0.90 mmol) dissolved in 5.0 mL toluene was added under Ar to 25 mL toluene solutions containing 1-hexene (1.58 g, 18.7 mmol) and Tris(pentafluorophenyl)boron (0.024 g, 0.047 mmol). The reaction mixture was quenched with 3 mL of d_4-CD_3OD at a selected time point corresponding to ca. 50% completion. An identical reaction to that described was initiated and at the same selected time for the above reaction quench; here an additional equivalent of labeled Zr[tBu-ON^{THF}O]d^7-Bn_2 (0.073 g, 0.90 mmol) in 5 mL was added to the ongoing polymerization reaction. This reaction was quenched with 3 mL of d_4-CD_3OD in its entirety at ca. 80% conversion. In a second batch with added labeled precatalyst, the polymerization reaction was run until completion before quenching with d_4-CD_3OD at >90% conversion. The quenched solutions from each of the above reactions were worked up and analyzed for monomer consumption by ^{1}H NMR, active site counting by ^{2}H NMR, extent of deuterium incorporation into the poly hexene by ^{2}H NMR, and MWD of the resulting polymer by GPC, as described previously.[7]

Kinetic Modeling Method. In previous work, we have determined the time-dependent concentrations of all species by solving the set of coupled nonlinear ordinary differential equations (ODEs) that result from mass action kinetics for a given polymerization mechanism.[7] However, ODE methods are significantly more difficult when the number of chemical species is combinatorially large, as is the case when there is the association/dissociation of two polymer species that occurs via a BNC-mediated reaction. Specifically, the number of distinct BNC species is the number of all possible combinations of all chain lengths—a computationally intractable number even for the massively parallelized ODE solver that we have developed.[20] Thus, we have developed a new solution algorithm based upon Dynamic Monte Carlo (DMC) methods[21] that is mathematically equivalent to the more traditional ODE formulation. The implementation of the DMC method employs the Gillespie's algorithm[21] for which a new computer code has been developed. Determination of the optimal set of the rate constants needed to fit a given mechanism to multiresponse experimental data employs the Nelder−Mead (i.e., simplex) optimization procedure.[22] A complete discussion of the formulation, DMC algorithm, and the Nelder−Mead optimization procedure is given in the Supporting Information.

RESULTS

The 1-hexene polymerization using zirconium amine bis-phenolate catalyst, Zr[tBu-ON^{THF}O]Bn2 has been investigated previously with stoichiometric amounts of activator;[7b] herein, the effect of substoichiometric activator concentration is the primary focus. The conditions studied are listed in Table 1, where Case 1 is the stoichiometric condition. A caveat is that the current experimental procedure involves first mixing activator and the precatalyst, and then adding monomer,

dx.doi.org/10.1021/cs500021g | ACS Catal. 2014, 4, 1162−1170

whereas previously the precatalyst was added to the mixture of activator and monomer.

Activation Analysis. The catalyst/activator system under study has been previously shown to activate quickly and cleanly under both stoichiometric and a slight excess activator in neat 1-hexene.[16,17] Under these conditions, polymeryl exchange experiments showed that each catalytic species present in the system acts independently with no communication between different catalytic species.[16] Spectroscopic evidence for this conclusion is furnished by (i) the immediate conversion of the precatalyst to two sharp benzylic ^{1}H signals (δ 2.89 and 2.62 ppm) and (ii) the clean conversion of the ^{19}F signals of the borane activator (δ −128.4, −143.2, and 160.6 ppm) into the borate counteranion (δ −131.6, −164.8, and 167.8 ppm). In situations where the precatalyst to activator ratio is more than 1 (i.e., the activator is limiting), the conversion of borane to the borate counteranion remains clean. However, the ^{1}H spectrum of the resulting reaction mixture shows significant line broadening of the two benzyl signals, indicating a dynamic process in which the benzyl groups are rapidly exchanged between two catalytic species (Figure S4).

Kinetics of Polymerization. For every condition in Table 1, six experiments were carried out: three experiments to prespecified monomer conversions and three to full conversion. Time-dependent monomer consumption was monitored for the three experiments proceeding to full conversion; end point monomer consumption was measured for every experiment. The MWD of polymers was obtained via GPC at the end of all six experiments. The active site counts were obtained at the end of the three reactions to prespecified monomer conversions as shown in Figure 2. The active site count was determined by quenching with d_4-methanol and performing ^{2}H NMR measurement of the concentration of chains with deuterated end groups using established methods.[7] The sites that have undergone 1,2-insertion are defined as primary sites, and the sites that have undergone 2,1-misinsertion are defined as secondary sites. Representative examples of the MWD at full monomer conversion are shown in Figure 3. The concentrations of vinyl end groups were shown to be negligible for this catalyst system.[7b]

Table 1. Initial Conditions of NMR Scale Experiments—"C" − Pre-Catalyst, "A" − Activator, "M" − Monomer

case	$[C]_0$ (mM)	$[A]_0$ (mM)	$[A]_0/[C]_0$	$[M]_0$ (mM)
1	3.0	3.3	1.1	600
2	3.0	1.5	0.5	600
3a	3.0	0.75	0.25	600
3b	6.0	1.5	0.25	1200

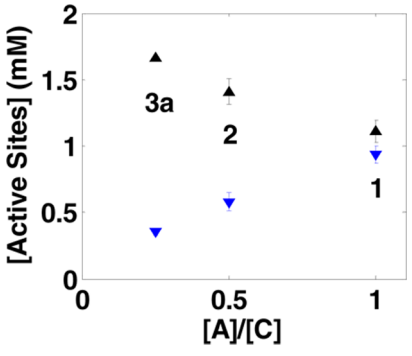

Figure 2. Active site counts of quenched NMR scale reactions 1, 2, 3a. Black up-pointing triangles: primary site counts; blue down-pointing triangles: secondary site counts.

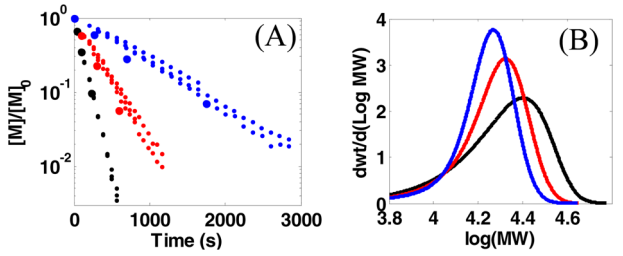

Figure 3. (A) Comparison of NMR scale and quenched NMR scale reactions 1, 2, 3a. Initial concentrations are shown in Table 1. Black: case 1; red: case 2; blue: case 3. (B) Corresponding end point MWDs.

When substoichiometric amounts of activator were used, the following features of the polymerization reaction emerged, as shown in Figures 2 and 3:

1. The consumption rate decreases with a decrease in activator amount.
2. The measured total amounts of active sites are almost the same for Cases 1, 2, and 3a. Although the total amount of active sites remains nearly constant, the amount of secondary sites decreases with decreasing amounts of activator, and the amount of primary sites increases as shown in Figure 2.
3. Despite the measured total amount of active sites being constant, the MWD in the substoichiometric cases surprisingly shifts toward lower molecular weights and becomes narrower (i.e., in Figure 3B, the PDIs for Case 2 is 1.17 and 3a is 1.12 vs PDIs of 1.29 for stoichiometric conditions, Case 1).

Kinetic Analysis. The natural point of departure for a detailed kinetic model is the set of elementary reactions that was previously developed to describe the polymerization reaction under stoichiometric activator conditions.[7a] The set consists of initiation, propagation, misinsertion, and recovery, as shown in Scheme 1, where the active catalyst is denoted as C*, primary active site as R_i, secondary active site as P_i, and the index i indicates the length of the polymer chain. In what follows this mechanism is referred to as Base Model. In light of Points 1−3 above, the Base Model predicts that when there is less activator, less precatalyst is activated, resulting in lower number of active sites and consequently higher molecular weight polymers. However, the experimental data in Figures 2 and 3 clearly contradict these predictions, where experimentally the molecular weight decreases and the number of active sites remains constant as the activator concentration is decreased. Including chain transfer reactions does lower the molecular weight; however, this also results in significant broadening of the MWD, which is not observed experimentally. *The Base Model cannot describe experiments with substoichiometric activator concentrations.*

Assuming that each activator molecule is responsible for the formation of a single active site, the amount of active sites should not exceed the initial amount of activator. However, in Cases 2 and 3a, the amount of active sites measured by NMR (i.e., the sum of the primary and secondary sites) is 2.1 mM in both cases, which is higher than the 1.5 mM or 0.75 mM of

dx.doi.org/10.1021/cs500021g | ACS Catal. 2014, 4, 1162−1170

Scheme 1. Elementary Kinetic Steps Included in the Base Model

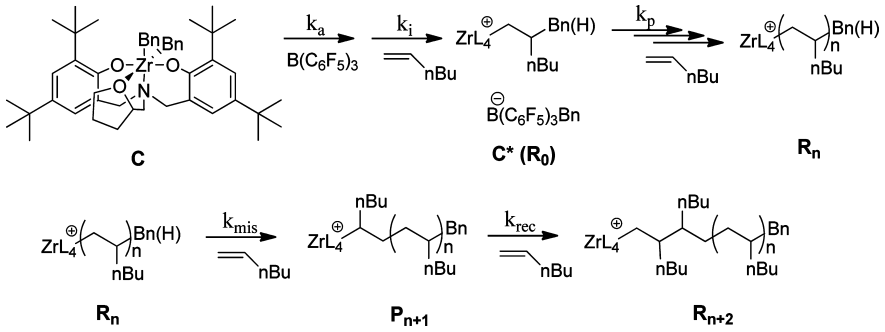

activator used in 2 and 3a, respectively. This leads to the idea of *reversible activation*, which allows for activating more precatalyst than the nominal amount of activator. The reversible activation model assumes that the activator can transfer between an actively polymerizing catalyst complex and an inactive chain, where the activator transfer reactivates the inactive chain for further polymerization but inactivates the previously growing catalyst−polymer complex. A detailed analysis of the Reversible Activation Model is given in the SI, where this model does have some beneficial features. Nevertheless, the ^{19}F NMR results described in the Activation Analysis section eliminates this model, because the model does not distinguish between stoichiometric and substoichiometric cases, whereas the broadening of benzyl ligand NMR lines is observed under the substoichiometric conditions versus sharp peaks under stoichiometric conditions.

Ligand Transfer Model. The difference between stoichiometric and substoichiometric activator conditions is the presence of unactivated precatalyst. The Ligand Transfer Model assumes that the precatalyst is activated by direct transfer of the benzyl ligand (Bn) from the precatalyst to the active catalyst via the formation of a binuclear complex (BNC). Unlike the case of reversible activation, ligand transfer will not take place under stoichiometric conditions, because there is no excess precatalyst.

BNC formation/dissociation is assumed to take place via Scheme 2, where L_4 denotes the 4-fold ligated [tBu-ON^{THF}O]

Scheme 2. Associated Elementary Kinetic Steps of the BNC Formation

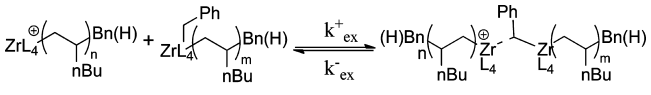

moiety. A BNC consists of one active catalytic complex (R_i or P_i) and one inactive catalytic complex, denoted here as Bn−R_j or Bn−P_j. When Bn shifts from the inactive catalyst to the active one in the BNC, the inactive catalyst becomes active and vice versa. The mass action equation for the reaction in Scheme 2 is given by eq 1.

$$R_i + \text{Bn}-R_j \underset{k_{ex}^-}{\overset{k_{ex}^+}{\rightleftharpoons}} R_i-\text{Bn}-R_j \quad (1)$$

$$P_i + \text{Bn}-P_j \underset{k_{ex}^-}{\overset{k_{ex}^+}{\rightleftharpoons}} P_i-\text{Bn}-P_j \quad (1')$$

$$CC^* \xrightarrow{k_{i,BNC}} R_1 + C \quad (2)$$

$$C^* - \text{Bn}-R_i \xrightarrow{k_{i,BNC}} R_1 + \text{Bn}-R_i \quad (3)$$

Equations 1 and 1′ use a compact notation where the activated catalyst C* is denoted as R_0, and the precatalyst C is denoted as Bn−R_0.

Introduction of the BNC complex in the mechanism leads to several questions that need to be addressed: Are both primary and secondary active sites capable of forming the BNC (does eq 1′ occur)? Is the BNC formation reversible? Does the BNC propagate, and what is the propagation rate constant? Lastly, can a BNC that consists of the activated catalyst and a precatalyst (i.e., C−C*) be initiated, and if this is possible, what is the rate constant of eqs 2 and 3? The answer to each of these questions will result in different versions of the Ligand Transfer Model. We summarize and eliminate various alternative models, where the detailed analysis is given in the SI.

1. The case that both primary and secondary active sites form BNC can be dismissed, because it is not selective with respect to the primary and secondary sites. As explained in the SI, if the BNC is formed by both primary and secondary sites with equal probability, the ratio of primary to secondary sites will not change with the activator-to-catalyst ratio. This is in obvious contradiction with the experimental observation shown in Figure 2. If on the other hand, the BNC is formed predominantly by the primary sites, their relative abundance can be explained. In other words, the secondary site count decreases with the activator amount normally, as it would in the absence of BNC formation. The primary site count would have behaved in the same way if not for the additional activation channel afforded by the BNC. In formal terms, this implies that eq 1′ does not occur and hence the species Bn−P_j do not form.
2. The BNC formation has to be reversible, otherwise one activator can only activate two precatalysts at most. Specifically, if the BNC formation was not reversible, then at a 1:4 [A]:[C] ratio (i) only one-half (instead of all) of the catalyst would grow chain, hence the active site counts would be lower than the observed value (i.e., 70%, see Figure 2), and (ii) the molecular weight would be much higher in contradiction to the experimental data.
3. If the initiation rate of BNC k_{i_BNC} is no faster than k_i, the shift of the MWD to lower values with a decrease in activator-to-catalyst ratio seen in Figure 3B is not fully predicted as explained in the SI. However, when k_{i_BNC} is much faster than k_i, the shift in the MWD is captured.

dx.doi.org/10.1021/cs500021g | ACS Catal. 2014, 4, 1162−1170

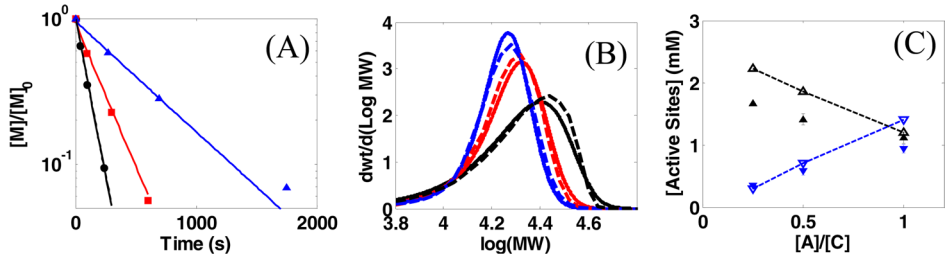

Figure 4. Ligand Transfer Model predictions of NMR scale reactions 1 (black), 2 (red), 3a (blue) based on Model 3.3. (A) Monomer consumptions. Data: symbols; predictions: lines. (B) End-point MWDs. Data: solid; predictions: dashed. (C) Active site counts of reactions 1, 2, and 3. Data: black up-pointing; triangles: primary site counts; blue down-pointing triangles: secondary site counts; predictions: dashed lines with unfilled triangles.

Table 2. Optimized Rate Constants for Ligand Transfer Model

k_i (M^{-1} s^{-1})	k_p (M^{-1} s^{-1})	k_{mis} (M^{-1} s^{-1})	k_{rec} (M^{-1} s^{-1})	k_{ex}^{+} (M^{-1} s^{-1})	k_{ex}^{-} (s^{-1})	K_{ex} (M^{-1})	k_{i_BNC} (M^{-1} s^{-1})	$\frac{[BNC]}{[A]_0}$ at $\frac{[A]_0}{[C]_0} = \frac{1}{2}$	$\frac{[BNC]}{[A]_0}$ at $\frac{[A]_0}{[C]_0} = \frac{1}{4}$
0. 08	8.0	0.054	0.040	400	20	20	12	3%	4%

Thus, the Ligand Transfer Model involving eqs 1−3 has the appropriate mechanistic structure to describe all the data sets with different activator-to-catalyst ratios. As shown in Figure 4, the agreement between the model predictions and the experimental data is quite good. The optimized rate constants are given in Table 2.

Based on the optimized rate constants shown in Table 2, the ratio of BNC concentration to the total catalyst concentration is very low under substoichiometric conditions. Consequently, unless the BNC propagation rate is 2 orders of magnitude or more higher than k_p, it has little effect on the monomer consumption rate and the MWD. Thus, for simplicity we will assume that the propagation rate by BNC was equal to k_p of the zwitterionic catalyst.

In order to experimentally validate the Ligand Transfer Model, a qualitatively different experiment was developed, where a second shot of precatalyst was added at 44% conversion (feed at 0 s: $[C]_0$ = 3.0 mM, $[A]_0$ = 1.5 mM, $[M]_0$ = 0.60 M; at 157 s: $[C]_1$ = 3.0 mM). Deuterated benzyl ligands were used for this second shot of precatalyst. It was observed from NMR that a fraction of the final polymer products contained deuterated benzyl, indicating that the added precatalyst activates and participates in polymerization despite seemingly having no activator left by which to be activated. The number of secondary sites decreases, and the number of primary sites increases after the second precatalyst addition is made. Furthermore, after the addition of precatalysts in the middle of the reaction, a second peak appears in the MWD, as shown in Figure 5. The rate of monomer consumption is not affected by the addition of precatalyst.

Examining the results in Table 2, the k_{i_BNC} initiation rate constant is significantly higher than the standard initiation rate constant k_i. To validate this prediction of the Ligand Transfer Model, we carried out two polymerization experiments with low monomer-to-activator ratio (5:1), where the activator to precatalyst ratio was in one case 1:1 and in the other case 1:4 (i.e., substoichiometric). Low monomer-to-activator/catalyst ratio experiments are sensitive to the ratio of the initiation rate to the propagation rate allowing more accurate determination of the initiation rate.[7c] Specifically, in a typical case of the k_i to k_p ratio of approximately 1:100 and a monomer-to-catalyst ratio of 100 or higher, the initiation is fast on the experimentally accessible time scale, where the number of growing chains reaches a maximum and then remains constant, as shown

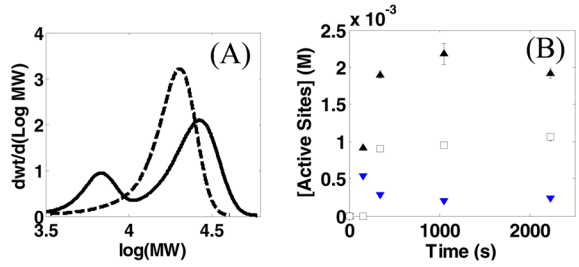

Figure 5. Batch scale experiment with additional shot of precatalyst (3.0 mM) at 44% conversion. Initial conditions: $[C]_0$ = 3.0 mM, $[A]_0$ = 1.5 mM, $[M]_0$ = 0.60 M. (A) Active site counts and d_7-benzyl incorporation (sqares) of catalyst pulse batch scale reactions. Black up-pointing triangles: primary site counts; blue down-pointing triangles: secondary site counts. (B) MWDs at 44% (dashed) and at 100% (solid) conversion.

schematically by the dotted line in Figure 6B. On the other hand, in the case of the monomer-to-catalyst ratio of 5:1, the

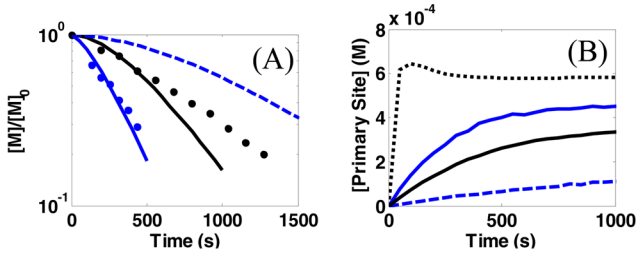

Figure 6. Initiation kinetics under low monomer-to-catalyst ratios. Initial conditions: $[A]_0$ = 1.5 mM, $[M]_0$ = 7.5 mM, $[C]_0$ = 1.5 mM (black) and 6.0 mM (blue). (A) Monomer consumptions. Symbols are data, curves are predictions. (B) Predictions of primary site concentration. Rate constants are reported in Table 2, except that k_{i_BNC} = 0 for blue dashed curve.

initiation continues in the course of the entire polymerization reaction, resulting in a pronounced induction period seen in the monomer consumption curve (solid black curves in Figure 6A,B). Data in Figure 6A present the comparison between the cases of stoichiometric and substoichiometric activator to precatalyst ratios (with the activator amount being fixed). In the substoichiometric case, the BNC is formed. Now if the BNC did not participate in the initiation, it would effectively act as a deinitiator. This is because when the BNC is formed by an

dx.doi.org/10.1021/cs500021g | ACS Catal. 2014, 4, 1162−1170

active site and a precatalyst and then is dissociated as an uninitiated active site and a neutral catalytic species, neither of them can propagate. As a result, it is predicted somewhat unexpectedly that if k_{i_BNC} is much slower than k_p, then the system with an excess amount of precatalyst would consume monomer at a much slower rate than the one with the lower amount of precatalyst. This prediction is shown schematically as a dashed blue line in Figure 6. This of course is not observed experimentally, as evidenced by Figure 6A, where the consumption in the substoichiometric case is in fact faster than that in the stoichiometric case (blue circles vs black circles). By the above reasoning this can only be the result of the k_{i_BNC} initiation rate by the BNC being fast, much faster than k_i.

To summarize, the simplest reaction mechanism capable of accounting for the experimental results was determined to be Schemes 1 and 2. In addition to predicting the data in Figure 4 (Cases 1, 2, and 3a in Table 1), the Ligand Transfer Model successfully describes the rest of the data (including Case 3b) and in particular the time evolution of MWD shown in Figure 7. The only unsatisfactory prediction is for the lowest (29%)

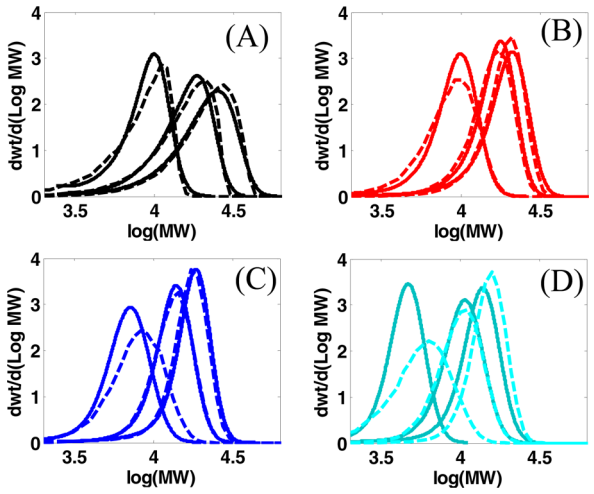

Figure 7. Modeling predictions of NMR scale reactions 1 (black), 2 (red), 3a (blue), 3b (cyan) based on Model 3.3. (A) MWDs at 35%, 65%, 91% conversion, (B) MWDs at 43%, 77%, 94% conversion, (C) MWDs at 41%, 72%, 93% conversion, (D) MWDs at 29%, 56%, 86% conversion. Data: solid; predictions: dashed.

conversion in Case 3b (Figure 7D). A possible explanation for this discrepancy is that the light scattering d*n*/d*c* value decreases from the constant value when the molecular weight is low ($M_w \leq 5000$ for the lowest peak in Figure 7C,D). The overestimation of this value results in the underestimation of the sample molecular weight. The catalyst participation (i.e., fraction of the of precatalyst being active in the reaction) for this system is approximately 90% as determined from fitting the data using the method reported previously.[7] This is attributed to experimental error or a small amount of impurities.

DISCUSSION

A selected zirconium amine bis-phenolate catalyst system has been studied, where a rich kinetic data set including the evolution of MWD has been collected for a wide range of initial conditions with a focus on the substoichiometric amounts of activator. As previously reported,[7b] the mechanism of 1-hexene polymerization for this catalyst using a stoichiometric amount of activator consists of the following elementary reaction steps: initiation, normal propagation, misinsertion, and recovery. However, under substoichiometric amounts of activator, additional elementary steps are needed to describe the data that involve the formation of a binuclear complex (BNC). Validation of the BNC-based mechanism was obtained via (i) NMR scale polymerizations listed in Table 1, where the active site counts and MWD both indicate the catalyst participation is the same even as the activator to catalyst ratio is varied and (ii) the use of a novel experimental technique wherein a labeled precatalyst was injected into a normal polymerization reaction at approximately ∼50% conversion, resulting in instantaneous activation of all incoming precatalyst. As the reaction proceeds, a second peak appears in the MWD that initially has a lower molecular weight, which is the result of chains growing on the newly formed active sites.

Comprehensive kinetic modeling yielded values of the rate constants for all the elementary reactions, including the ones involving the BNC, given in Table 2. Although the literature has ample support from empirical observations and semi-quantitative measurements that groups such as −Cl and −Me can participate in degenerative transfer,[12] we present a quantitative measure of the rate constants that govern the association and dissociation of the complex leading to degenerative transfer and for the first time demonstrate ligand transfer with the benzyl group.

The ligand exchange process in this system is found to be rapid as evidenced by significant line broadening of the two benzylic signals in the ^{1}H spectrum. By examining the data in Table 2, one can see that the formation rate of BNC (i.e., k_{eq}^{+}) is extremely fast as is the interconversion of species R_n and Bn−R_n, on the time scale of the other elementary steps contained within the mechanism. The dissociation rate of BNC, k_{eq}^{-}, is also fast, given that it is a first order rate constant. The rapid dissociation of this complex indicates that it is an unstable complex. Therefore, the concentration of BNC at any moment is much lower than the concentration of R_n. This is in agreement with the literature[12] conclusion that BNC compounds are unstable and no isolated crystal structure has been obtained; consequently, the exchange rate could only be qualitatively estimated in previous work.[12] In contrast, the quantitative kinetic modeling methodology presented here provides quantitative analysis of the dynamics of the BNC. Two major conclusions from this work are the following:

1. With the decrease in activator, there is a systematic decrease in misinserted sites and an increase in normally inserted sites. To account for this effect, the Ligand Transfer Model postulates that the secondary active sites P_n (formed by misinsertion) cannot form the BNC. A possible explanation is that the large side group of the misinserted chain hinders the ability of the benzyl ligand to bridge the two zirconium centers. *By effectively shutting down the misinsertion pathway (i.e., the formation of P_n), the use of substoichiometric amounts of activator causes the $Zr[^tBu\text{-}ON^{THF}O]Bn_2$/ $B(C_6F_5)_3$ system to approach that of a living polymerization.*
2. Initiation via BNC is much faster than the normal initiation of a single active catalyst. This is likely due to the anion being previously displaced by the incoming precatalyst and also due to the two metal centers present in BNC not being as tightly associated as in the case of a normal zwitterion pair catalyst. *As a result, the MWD of*

dx.doi.org/10.1021/cs500021g | ACS Catal. 2014, 4, 1162−1170

the polymer is systematically lowered with decreasing activator concentration.

Note that the mechanism developed in this paper can be used to analyze the data of Sita et al.[12] with the caveat that misinsertion does not occur in the first place for that system. The details of the analysis are given in the SI, and the main results are summarized in Table 3. Catalyst participation is determined to be 68% based on M_n versus $[M]_0/[Zr]_{tot}$ dependence, which for the case of living polymerization gives the amount of growing chains.

Table 3. Modeled Results of Sita's $Cp^*ZrMe_2[N(tBu)C(Me)N(Et)]/[B(C_6F_5)_4]$ System

k_p ($M^{-1}s^{-1}$)	K_{ex} (M^{-1})	k_{ex}^+ ($M^{-1}s^{-1}$)	$\frac{[BNC]}{[A]_0}$ at $\frac{[A]_0}{[C]_0} = \frac{1}{2}$	$\frac{[BNC]}{[A]_0}$ at $\frac{[A]_0}{[C]_0} = \frac{1}{4}$
19.6	111.5	$>3 \times 10^3$	10%	25%

Similar to the current system, the system of Sita et al.[12] is characterized by an association rate of BNC which is much faster than k_p. Sita et al. reasoned that the BNC does not propagate. Specifically, they observed that the rate of monomer consumption linearly decreased with an increase in the amount of precatalyst when keeping the activator concentration constant. Specifically, assuming that the excess of precatalyst results in formation of BNC; if the BNC propagates at the same rate as the normal active site, then the consumption rate will not change; because this is not the case, the BNC must be less active. The quantitative kinetic analysis developed in this paper is consistent with this conclusion, where the decrease in the observed consumption rate with increasing precatalyst concentration enables determination of the amount of the BNC. It is instructive to evaluate the ratio of the BNC concentration to the total amount of activator used, as this allows comparison across different systems. As shown in Table 3, the ratio of the concentration of BNC to the total cation concentration for the Sita catalyst is 10% and 25% at the 1/2 activator and 1/4 activator condition, respectively. These values are significantly higher than their counterparts for our $Zr[tBu\text{-}ON^{THF}O]Bn_2/B(C_6F_5)_3$ system given in Table 2 with 3% and 4% at the 1/2 activator and 1/4 activator condition, respectively. Finally, the Ligand Transfer Model shows that the concentration of BNC is not a linear function of the excess amount of precatalyst, where with addition of more precatalyst, the decrease in consumption rate becomes less significant.

CONCLUSIONS

A comprehensive kinetic study of the $Zr[tBu\text{-}ON^{THF}O]Bn_2/B(C_6F_5)_3$ system under substoichiometric activator conditions has been completed, where decreasing the amount of activator causes (i) the rate of monomer consumption to decrease and (ii) the MWD to narrow and shift to lower values. Using quantitative kinetic analysis, a Ligand Transfer Model was developed that is capable of describing the diverse data set. This mechanism includes the formation of the binuclear complex (BNC) consisting of the neutral catalytic species and an active site connected via degenerative transfer of benzyl ligand. Bridging via methyl and chloral ligands has been previously postulated,[12,15] but not bridging via a benzyl ligand, which has been argued to be infeasible.[15] The BNC can be formed when precatalyst species react with an active catalyst, thereby providing a second channel for activation. *The most significant finding of this study was that the BNC is only formed by the normally inserted active sites and not by misinserted sites, resulting in narrowing of the MWD of the polymer, as compared to the case of stoichiometric activator where the BNC is not formed.* Although under the conditions studied the BNC concentration is small compared to the concentration of active sites due to the small equilibrium constant of BNC formation, it is shown to play an important role in initiation, which is faster via the BNC. This results in the experimentally observed lower and narrower MWD of the resulting polymer.

ASSOCIATED CONTENT

Supporting Information

The SI includes (i) synthesis of ligand and precatalyst, (ii) a complete set of experimental procedures used to determine kinetic data for each system, and (iii) detailed kinetic modeling of all models considered. This material is available free of charge via the Internet at http://pubs.acs.org.

AUTHOR INFORMATION

Corresponding Authors

* (J.M.C.) caruther@purdue.edu.
* (M.M.A.) mabuomar@purdue.edu.

Author Contributions

All authors have given approval to the final version of the manuscript.

Notes

The authors declare no competing financial interest.

ACKNOWLEDGMENTS

Financial support was provided by the U.S. Department of Energy by grant no. DE-FG02-03ER15466. This research was supported in part by the National Science Foundation through TeraGrid resources provided by Purdue University under grant no. TG-CTS070034N. Computing resources were also provided by Information Technology at Purdue.

REFERENCES

(1) (a) Chen, E. Y.-X.; Marks, T. J. *Chem. Rev.* **2000**, *100*, 1391−1434. (b) Li, H.; Marks, T. J. *Proc. Natl. Acad. Sci. U.S.A.* **2006**, *103*, 15295−15302.

(2) Manz, T. A.; Phomphrai, K.; Medvedev, G. A.; Krishnamurthy, B. B.; Sharma, S.; Haq, J.; Novstrup, K. A.; Thomson, K. T.; Delgass, W. N.; Caruthers, J. M.; Abu-Omar, M. M. *J. Am. Chem. Soc.* **2007**, *129*, 3776−3777.

(3) (a) Krauledat, H.; Brintzinger, H. H. *Angew. Chem., Int. Ed.* **1990**, *29*, 1412−1413. (b) Piers, W. E.; Bercaw, J. E. *J. Am. Chem. Soc.* **1990**, *112*, 9406−9407. (c) Coates, G. W.; Waymouth, R. M. *J. Am. Chem. Soc.* **1991**, *113*, 6270−6271.

(4) Brintzinger, H. H.; Fischer, D.; Mullhaupt, R.; Rieger, B.; Waymouth, R. M. *Angew. Chem., Int. Ed. Engl.* **1995**, *34*, 1143−1170.

(5) Chen, Y.-X.; Metz, M. V.; Li, L.; Stern, C. L.; Marks, T. J. *J. Am. Chem. Soc.* **1998**, *120*, 6287−6305.

(6) (a) Jia, L.; Yang, X.; Stern, C. L.; Marks, T. J. *Organometallics* **1997**, *16*, 842−857. (b) Yang, X.; Stern, C. L.; Marks, T. J. *Organometallics* **1991**, *10*, 840−842.

(7) (a) Switzer, J. M.; Travia, N. E.; Steelman, D. K.; Medvedev, G. A.; Thomson, K. T.; Delgass, W. N.; Abu-Omar, M. M.; Caruthers, J. M. *Macromolecules* **2012**, *45*, 4978−4988. (b) Steelman, D. K.; Xiong, S.; Pletcher, P. D.; Smith, E.; Switzer, J. M.; Medvedev, G. A.; Delgass, W. N.; Caruthers, J. M.; Abu-Omar, M. M. *J. Am. Chem. Soc.* **2013**, *135*, 6280−6288. (c) Liu, Z. X.; Somsook, E.; White, C. B.; Rosaaen, K. A.; Landis, C. R. *J. Am. Chem. Soc.* **2001**, *123*, 11193−11207.

(8) Greszata, D.; Mardare, D.; Matyjasewki, K. *Macromolecules* **1994**, *27*, 638−644.

(9) (a) Muller, A. H. E.; Zhuang, R.; Yan, D.; Litvinenko, G. *Macromolecules* **1995**, *28*, 4326−4333. (b) Muller, A. H. E.; Yan, D.; Litvinenko, G.; Zhuang, R.; Dong, H. *Macromolecules* **1995**, *28*, 7335−7338.
(10) Hawker, C. J. *Acc. Chem. Res.* **1997**, *30*, 373−382.
(11) (a) Chong, Y. K.; Le, T. P. T.; Moad, G.; Rizzardo, E.; Thang, S. H. *Macromolecules* **1999**, *32*, 2071−2074. (b) Fukuda, T.; Moad, G.; Rizzardo, E.; Thang, S. H. *Macromolecules* **2001**, *34*, 402−408.
(12) (a) Zhang, Y.; Keaton, R. J.; Sita, L. R. *J. Am. Chem. Soc.* **2003**, *125*, 9062−9069. (b) Zhang, Y.; Sita, L. R. *J. Am. Chem. Soc.* **2004**, *126*, 7776−7777. (c) Kissounko, D. A.; Zhang, Y.; Harney, M. B.; Sita, L. R. *Adv. Synth. Catal.* **2005**, *347*, 426−432.
(13) (a) Chen, M.-C.; Roberts, J. A. S.; Marks, T. J. *J. Am. Chem. Soc.* **2004**, *126*, 4605−4625. (b) Neng, G.; Stern, C. L.; Marks, T. J. *J. Am. Chem. Soc.* **2008**, *130*, 2246−2261. (c) Rodriguez, B. A.; Delferro, M.; Marks, T. J. *Organometallics* **2008**, *27*, 2166−2168.
(14) Chen, Y.-X.; Marks, T. J. *Organometallics* **1997**, *16*, 3649−3657.
(15) Bochmann, M.; Lancaster, S. J. *Angew. Chem., Int. Ed. Engl.* **1994**, *33*, 1634−1637.
(16) Groysman, S.; Goldberg, I.; Kol, M. *Organometallics* **2003**, *22*, 3013−3015.
(17) Groysman, S.; Goldberg, I.; Kol, M.; Genizi, E.; Goldschmidt, Z. *Inorg. Chim. Act.* **2003**, *345*, 137−144.
(18) Younkin, T. R.; Connor, E. F.; Henderson, J. I.; Friedrich, S. K.; Grubbs, R. H. *Science* **2000**, *287*, 460−462.
(19) Tshuva, E. Y.; Gendeziuk, N.; Kol, M. *Tetrahedron Lett.* **2001**, *42*, 6405−6407.
(20) Cao, J.; Goyal, A.; Novstrup, K.; Midkiff, S.; Caruthers, J. *Int. J. Parallel Program.* **2009**, *37*, 127.
(21) Gillespie, D. T. *J. Comput. Phys.* **1976**, *22*, 403.
(22) Nelder, J.; Mead, R. *Comput. J.* **1965**, *7*, 308.